Journal of Coastal Research	23	5	1318–1323	West Palm Beach, Florida	September 2007

Nonlinear Wave–Wave Interactions in a Mistral Event

Mohamed A.K. Elsayed

Department of Engineering Science and Mechanics
Virginia Polytechnic Institute and State University
Mail Code (0219)
Blacksburg, VA 24061, U.S.A.
melsayed@vt.edu

ABSTRACT

ELSAYED, M.A.K., 2007. Nonlinear wave–wave interactions in a mistral event. *Journal of Coastal Research,* 23(5), 1318–1323. West Palm Beach (Florida), ISSN 0749-0208.

This study analyzes the detailed nonlinear wave–wave interactions during 6 hours of wave generation in a mistral event. Nonlinearity and phase coupling are computed using wavelet bicoherence, which is a new technique in analyzing wind–wave and wave–wave interactions.

Computations of wavelet bicoherence are conducted for the 13 continuous records of measured wave data. The phase coupling and nonlinear wave–wave interactions are shown to occur at different bicoherence levels, and these levels are different from one record to another. Furthermore, the study shows that there is an increase in nonlinear wave–wave interaction with time.

ADDITIONAL INDEX WORDS: *Morlet wavelet, continuous wavelet analysis, wavelet bicoherence.*

INTRODUCTION

Several studies have been carried out over a century to analyze wave generation by wind and wave growth in an attempt to understand these mechanisms. Among those studies are DONELAN and HUI (1990), KRAUS and BUSINGER (1994), LIGHTHILL (1962), MILES (1957, 1959a, 1959b, 1962, 1967), PHILLIPS (1957, 1958), and YOUNG and VERHAGEN (1996a, 1996b, 1996c).

Nonlinear wave–wave interactions are considered an important phenomenon; they produce a transfer of some wave energy from lower to higher wave periods as the spectrum grows.

The present study aims at analyzing nonlinear wave–wave interaction during wave growth. The main objectives of the paper are:

1. to analyze the development of nonlinear wave–wave interactions during 6 hours of wave generation using the data collected during a mistral event.
2. to compute wavelet bicoherence for the wind–wave time series in order to better understand the nonlinear wave–wave interactions that occur during wave growth.

DATA DESCRIPTION

The data used in this study were collected during the FETCH experiment (DRENNAN *et al.,* 2003). An ASIS buoy was deployed on 18 March 1998 and remained until 10 April 1998. This period corresponds to a mistral event, which is a regional wind occurring during conditions of high atmospheric pressure over western Europe, in particular over the Bay of Biscay, combined with a low-pressure system south of the Alps. The mistral event is characterized by a strong, steady, cold flow with near-surface wind speeds frequently in excess of 30 m/s (DRENNAN *et al.,* 2003). Thirteen records of the measured wave height were collected during the mistral event. Each record has a length of approximately half an hour (see Figures 1a through 13a).

DOI:10.2112/04–0378.1 received 26 January 2005; accepted in revision 1 June 2005.

ANALYSIS METHOD

Continuous Wavelet Analysis

The continuous wavelet transform $W(a, \tau)$ of a function $h(t)$ is defined as

$$W(a, \tau) = \int_{-\infty}^{+\infty} h(t)\psi^*_{a,\tau}(t)\, dt \tag{1}$$

where a and τ are scale and time variables respectively, and $\psi_{a,\tau}$ represents the wavelet family generated by continuous translations and dilations of the mother wavelet $\psi(t)$, and $\psi^*_{a,\tau}$ is the complex conjugate of $\psi_{a,\tau}$. These translations and dilations are obtained by

$$\psi_{a,\tau} = \frac{1}{\sqrt{a}}\psi\left(\frac{t - \tau}{a}\right). \tag{2}$$

Following TORRENCE and COMPO (1998) and ADDISON (2002), the complex Morlet wavelet (MORLET, 1981) to be implemented in this study is defined as:

$$\psi(t) = \pi^{-1/4}e^{iw_o t}e^{-t^2/2}. \tag{3}$$

In this definition, w_o is chosen to be 6.0 to approximately satisfy the wavelet admissibility condition (FARGE, 1992).

TORRENCE and COMPO (1998) developed a code for computing the continuous wavelet transform of the time series of

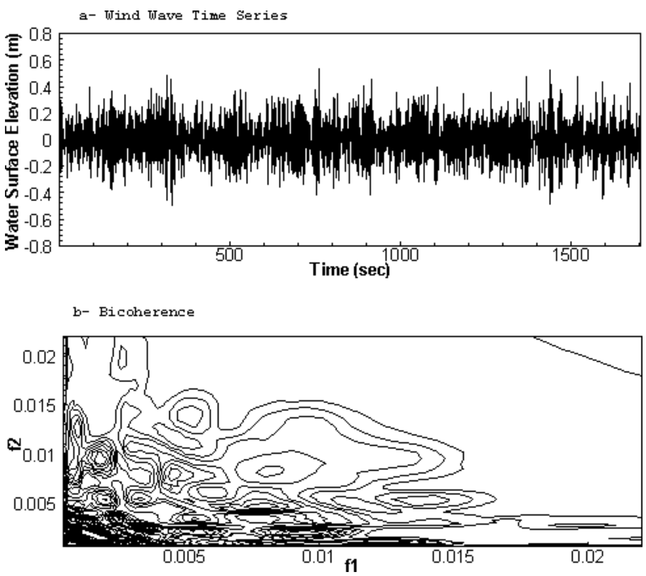

Figure 1. Wind–wave time series and corresponding wavelet bicoherence (record 1).

the signal. In this work, the code was modified to compute the cross-bispectrum and the wavelet cross-bicoherence.

Power spectrum

In order to have statistical stability, the wavelet power spectrum is integrated over a finite time interval (MILLIGEN *et al.,* 1995, 1997). The wavelet power spectrum is defined as

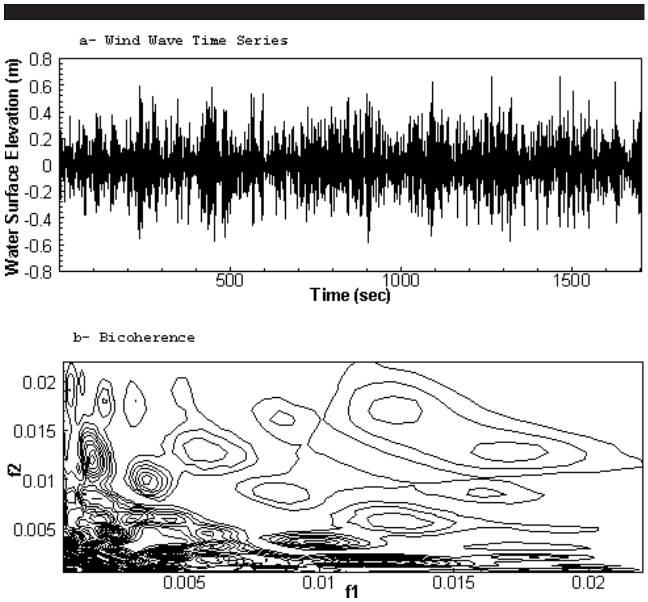

Figure 2. Wind–wave time series and the corresponding wavelet bicoherence (record 2).

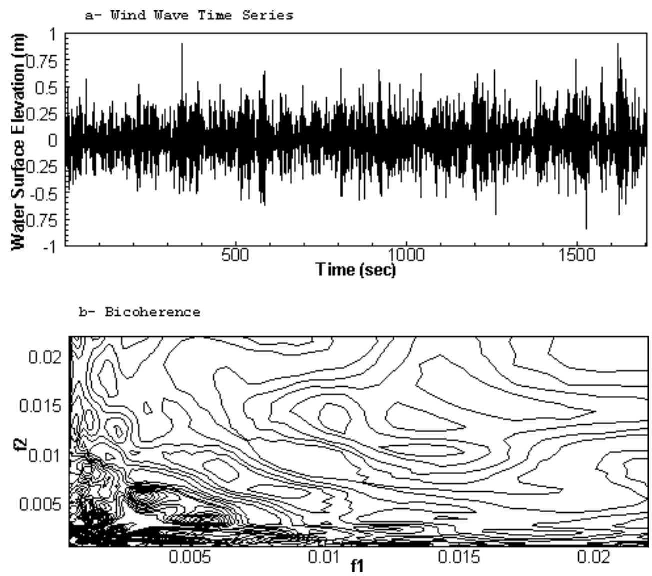

Figure 3. Wind–wave time series and corresponding wavelet bicoherence (record 3).

$$P_{xx}(a) = \int_T W_x^*(a, \tau) W_x(a, \tau)\, d\tau, \quad (4)$$

where $W_x(a, \tau)$ is the wavelet transform of the time series, $W_x^*(a, \tau)$ is the complex conjugate of wavelet transform of the time series, and T is a finite time interval.

Cross-spectrum

The wavelet cross-spectrum is defined as follows:

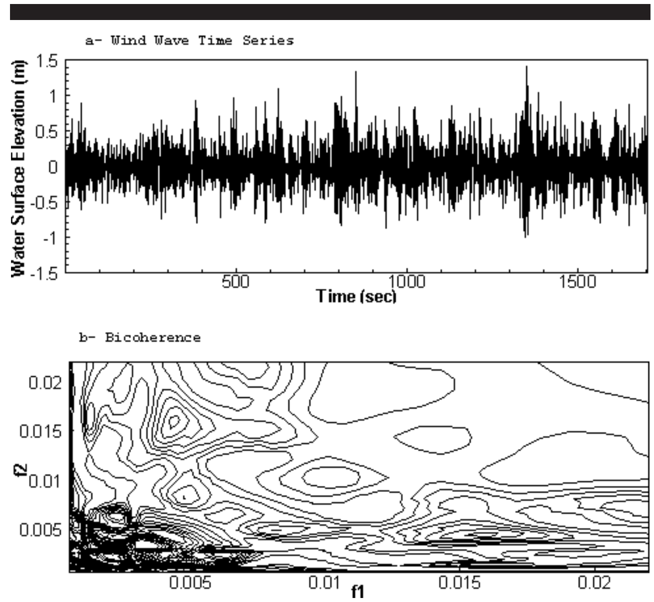

Figure 4. Wind–wave time series and corresponding wavelet bicoherence (record 4).

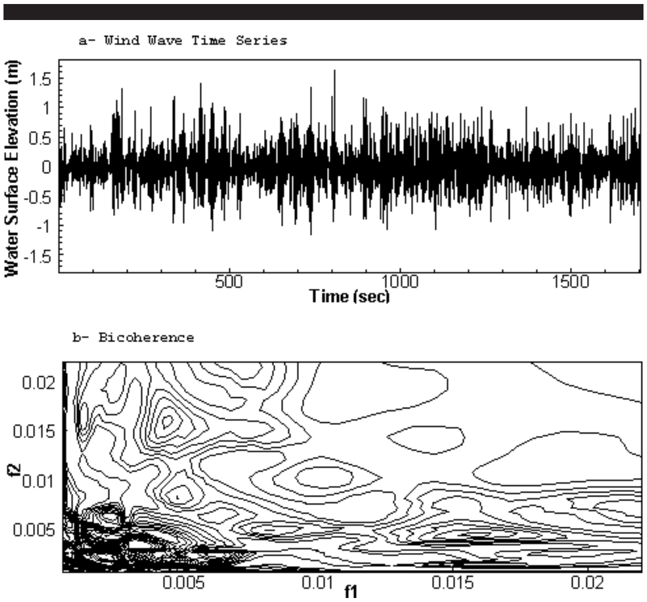

Figure 5. Wind–wave time series and corresponding wavelet bicoherence (record 5).

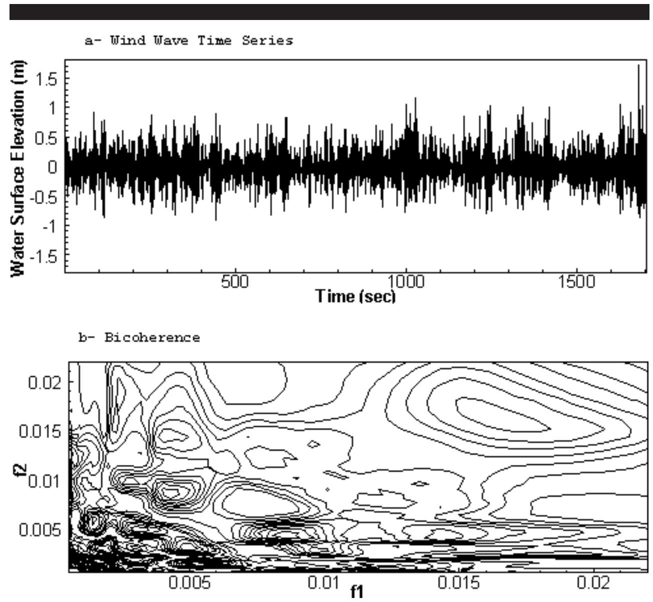

Figure 7. Wind–wave time series and corresponding wavelet bicoherence (record 7).

$$P_{xy}(a) = \int_T W_x^*(a, \tau) W_y(a, \tau)\, d\tau, \tag{5}$$

where $W_x^*(a, \tau)$ is the complex conjugate of wavelet transform of the first time series and $W_y^*(a, \tau)$ is the wavelet transform of the second time series.

It should be noted that the results of the cross-spectrum depend heavily on the fluctuations of the individual signals, because if one of the signals fluctuates less than the other, the effect of the more fluctuating signal will dominate in the resultant cross-spectrum (HAJJ, JORDAN, and TIELEMAN, 1998).

Linear Coherence

The normalized wavelet cross-spectrum is defined by

$$\mathrm{Coh}_{xy}(a) = \frac{|P_{xy}(a)|^2}{P_{xx}(a) P_{yy}(a)}, \tag{6}$$

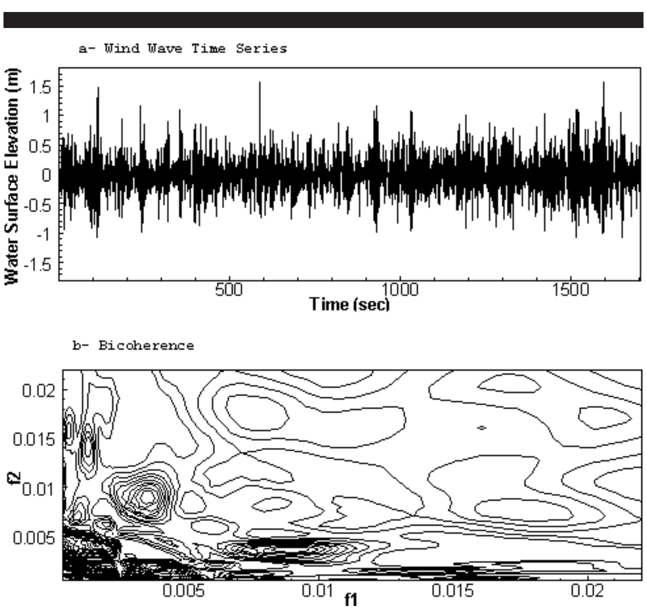

Figure 6. Wind–wave time series and corresponding wavelet bicoherence (record 6).

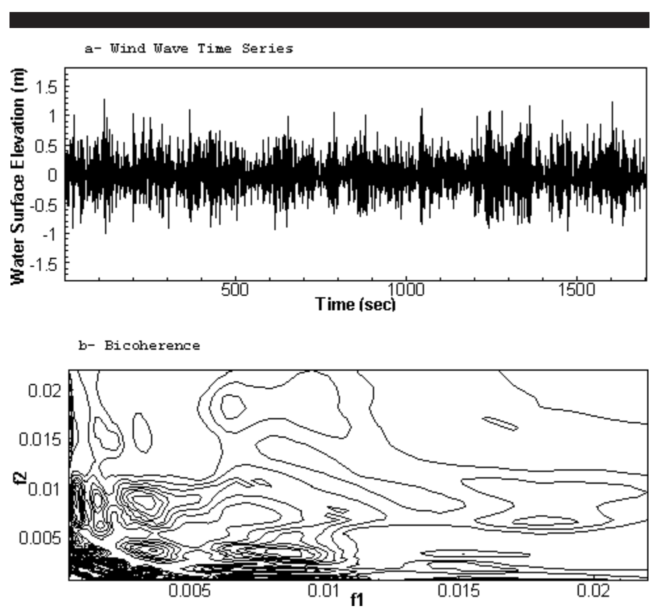

Figure 8. Wind–wave time series and corresponding wavelet bicoherence (record 8).

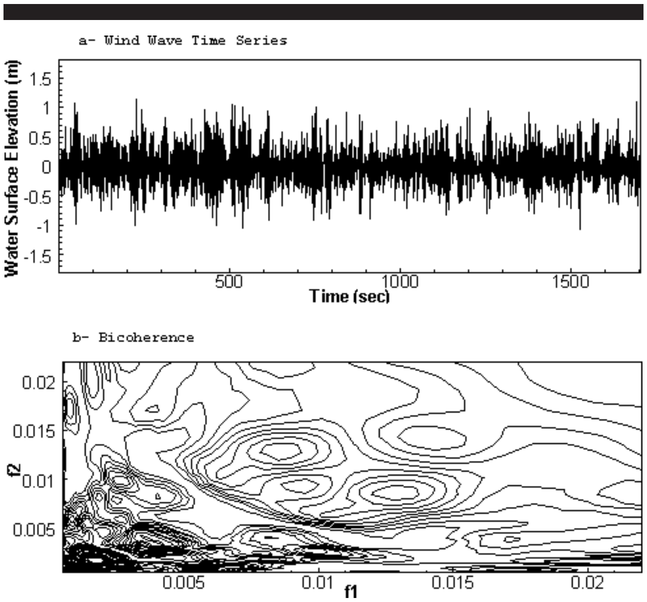

Figure 9. Wind–wave time series and corresponding wavelet bicoherence (record 9).

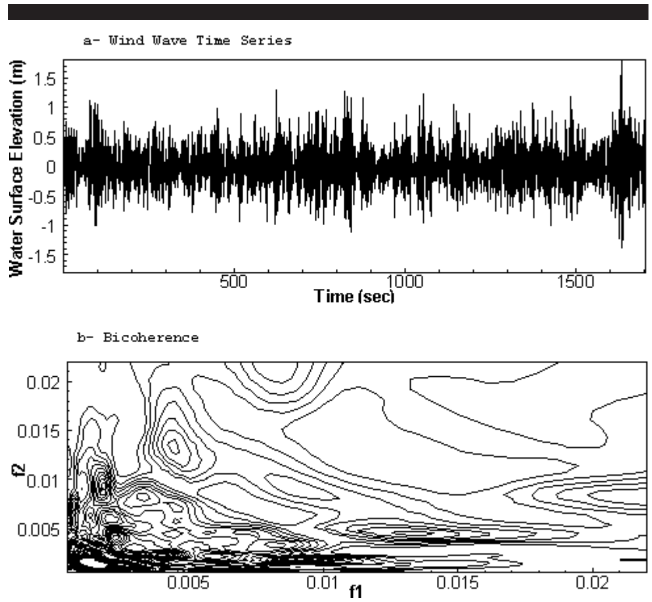

Figure 11. Wind–wave time series and corresponding wavelet bicoherence (record 11).

where $Coh_{xy}(a)$ is linear coherence between two time series, $P_{xx}(a)$ is the power spectrum of the first time series, $P_{yy}(a)$ is the power spectrum of the second time series, and $P_{xy}(a)$ is the cross-spectrum of the first and the second time series.

Cross-bispectrum

The wavelet cross-bispectrum is defined as follows:

$$B_{yxx}(a1, a2) = \int_T W_y^*(a, \tau) W_x(a1, \tau) W_x(a2, \tau)\, d\tau \qquad (7)$$

where $1/a = 1/a1 + 1/a2$ (frequency sum rule). The wavelet cross-bispectrum measures the amount of phase coupling in the time interval T that occurs between wavelet components of scale lengths $a1$ and $a2$ of $x(t)$ and wavelet component a of $y(t)$ such that the sum rule is satisfied (MILLIGEN *et al.,*

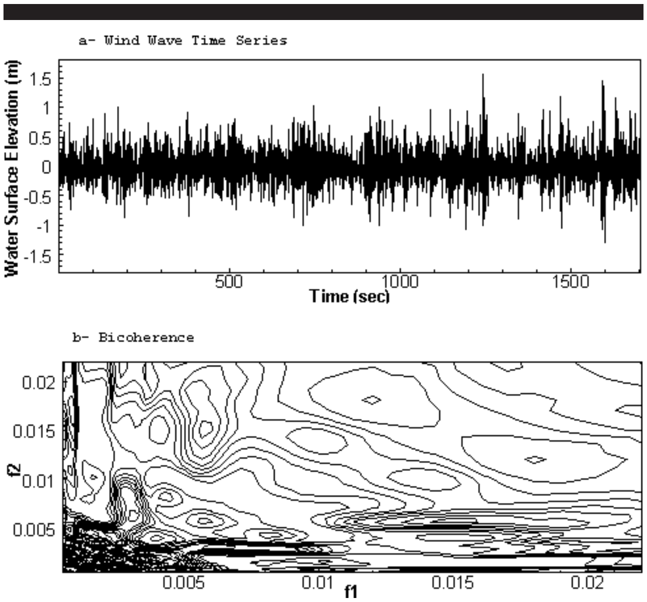

Figure 10. Wind–wave time series and corresponding wavelet bicoherence (record 10).

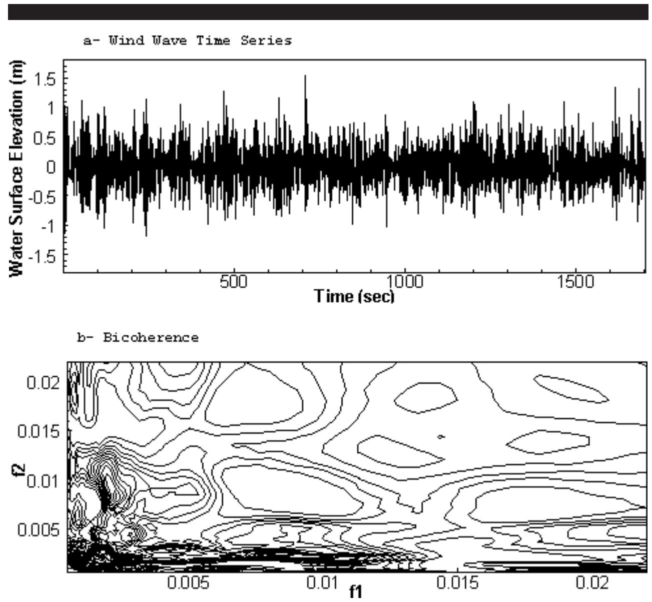

Figure 12. Wind–wave time series and corresponding wavelet bicoherence (record 12).

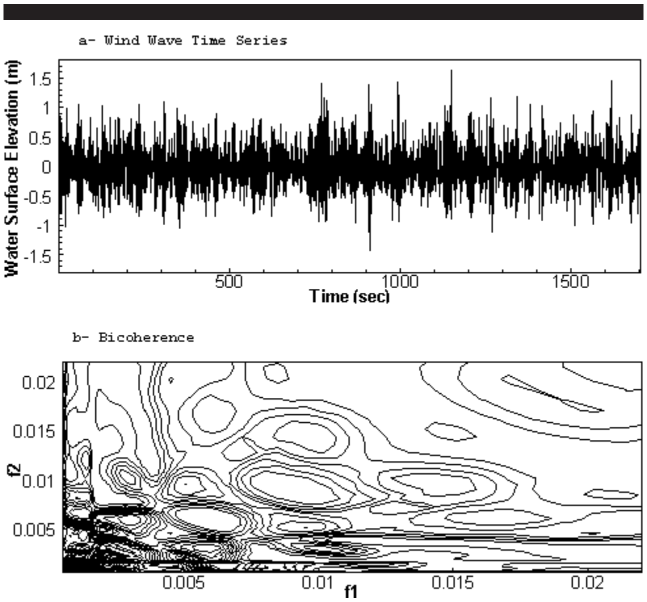

Figure 13. Wind–wave time series and corresponding wavelet bicoherence (record 13).

1995). The normalized squared wavelet cross-bicoherence is defined as:

$$[b_{yxx}(a1, a2)]^2 = \frac{|B_{yxx}(a1, a2)|^2}{\left[\int_T |W_x(a1, \tau)W_x(a2, \tau)|^2\, d\tau\right]\left[\int_T |W_y(a, \tau)|^2\, d\tau\right]}. \quad (8)$$

The wavelet bicoherence is a measure of phase coupling that occurs in a signal or between two signals. Phase coupling is defined as occurring when two frequencies, $f1$ and $f2$, are simultaneously present in the signal(s) along with their sum (or difference) frequencies, and the sum of the phases of these frequency components remains constant. The bicoherence measures this quantity and is a function of the two frequencies $f1$ and $f2$. The bicoherence is close to 1 when the signal contains three frequencies $f1$, $f2$, and f that satisfy the relation $f = f1 + f2$; if this relation is not satisfied, it is close to zero (Milligen *et al.,* 1995).

RESULTS AND DISCUSSION

To analyze the phase coupling and the nonlinear wave–wave interaction, wavelet bicoherence (wave and wave and wave) is computed for the 13 records of the measured wind–wave given in Figures 1a through 13a.

Figures 1b–13b give the computed wavelet bicoherence for the 13 wind–wave records, which were measured during six hours of wave growth in a mistral event. In computing the wavelet bicoherence, the time of integration is chosen to be from 1 to 1706 seconds, which represents the whole window of each record.

Figure 1b gives wavelet bicoherence for the first record. There are zones of the contours with high intensity, and these zones are indications of high values of bicoherence. The phase coupling and nonlinear wave–wave interactions are shown to occur at $f1 = 0.005$, 0.01, 0.014 and $f2$ equals to 0.001 to 0.01 and 0.005, as shown in Figure (1b).

Figure 2b shows that there is a phase coupling at $f1$ ranges from 0.001 to 0.005, 0.01 to 0.015, 0.019 and at $f2$ ranges from 0.001 to 0.005, at 0.013. Whereas, Figure 3b shows that phase coupling is occurring at $f1$ ranges from 0.001 to 0.02 and $f2$ ranges from 0.001 to 0.005 and at $f2 = 0.01$.

Figures 4b–13b show the development of nonlinear wave–wave interaction and phase coupling as the waves grow. It can be observed that phase coupling is occurring at different bicoherence levels and that there is an increase in nonlinearity in wave–wave interaction as the waves grow.

The nonstationary feature of the measured records of wind–wave is clearly shown; the wavelet bicoherence is different from one record to another because of this nonstationary feature.

The results obtained so far show that there is a phase coupling in all computed wavelet bicoherence for the combination of wave and wave and wave for the 13 measured records, and that the nonlinearity is developed in wave–wave interaction with time as the wave grows.

CONCLUSIONS

The main findings of the present study are summarized as follows:

- During wave growth when the spectrum grows, the nonlinear wave–wave interaction is a mechanism through which energy is transferred from lower to higher wave periods.
- Wavelet bicoherence, which is a new technique in the analysis of wind–wave and wave–wave interactions, is used to analyze nonlinear wave–wave interactions in order to analyze the nonlinearity and phase coupling taking place in the wave–wave interactions during wave generation.
- The details of the wave–wave interactions during wave growth are examined by computing wavelet bicoherence for the 13 records of the measured wind–wave data, which represent 6 hours of wave generation during a Mistral event.
- The study shows that the wave–wave phase coupling occurs over a particular range of frequencies, which is different from one record to another because of the nonstationary feature of the data set.
- This study adds a useful application of wavelet analysis and bispectrum analysis in detecting the phase coupling and nonlinear wave–wave interaction during wave growth.
- Finally, it is worth mentioning that the results of this study through the use of wavelet analysis could not be obtained by using classical Fourier analysis because of the nonstationary feature characterizing the wind–wave data set.

ACKNOWLEDGMENTS

The author would like to thank Dr. William Drennan from the Rosenstiel School of Marine and Atmospheric Science, University of Miami, Florida, for providing the data necessary for conducting the present study.

LITERATURE CITED

ADDISON, P.S., 2002. *The Illustrated Wavelet Transform Handbook: Introductory Theory and Applications in Science.* Bristol, United Kingdom: Institute of Physics Publishing, 349p.

DONELAN, M.A. and HUI, W.H., 1990. Mechanics of Ocean Surface Waves. *In*: GEERNAERT, G., AND PLANT, W. (eds.) *Surface Waves and Fluxes.* Dordrecht, Netherlands: Kluwer Academic Publishers, pp. 110–125.

DRENNAN, W.M.; GRABER, H.C.; HAUSER. D., and QUENTIN, C., 2003. On the wave age dependence of wind stress over pure wind seas. *Journal of Geophysical Research,* 108(C3), 8062–8075.

FARGE, M., 1992. Wavelet transforms and their application to turbulence. *Annual Review of Fluid Mechanics,* 24, 395–457.

HAJJ, M.R.; JORDAN, D.A., and TIELEMAN, H.W., 1998. Analysis of atmospheric wind and pressures on a low rise building. *Journal of Fluids and Structures,* 12, 537–547.

KRAUS E.B. and BUSINGER, J.A., 1994. Surface Wind Waves. In: *Atmosphere-Ocean Interaction.* New York: Oxford University Press, pp. 201–250.

LIGHTHILL, M.J., 1962. Physical interpretation of the mathematical theory of wave generation by wind. *Journal of Fluid Mechanics,* 14, 385–398.

MILES, J., 1957. On the generation of surface waves by shear flows. *Journal of Fluid Mechanics,* 3, 185–204.

MILES, J., 1959a. On the generation of surface waves by shear flows. Part 2. *Journal of Fluid Mechanics,* 6, 568–582.

MILES, J., 1959b. On the generation of surface waves by shear flows. Part 3: Kelvin-Helmholtz instability. *Journal of Fluid Mechanics,* 6, 583–598.

MILES, J., 1962. On the generation of surface waves by shear flows. Part 4. *Journal of Fluid Mechanics,* 13, 433–448.

MILES, J., 1967. On the generation of surface waves by shear flows. Part 5. *Journal of Fluid Mechanics,* 30, 163–175.

MILLIGEN, B.P.V.; HIDALGO, C.; SANCHEZ, E.; PEDROSA, M.A.; BALBIN, R.; GARCIA-CORTES, I., and TYNAN, G.R., 1997. Statistically robust linear and nonlinear wavelet analysis applied to plasma edge turbulence. *Review of Science Instruments,* 68(1), 967–970.

MILLIGEN, B.P.V.; SANCHEZ, E.; ESTRADA, T.; HIDALGO, C.; BRANAS, B.; CARRERAS, B., and GARCIA, L., 1995. Wavelet bicoherence: a new turbulence analysis tool. *Physics of Plasmas,* 2(8), 3017–3032.

MORLET, J., 1981. Sampling theory and wave propagation. Proceedings of the 51st Annual Meeting of the Society of Exploration Geophysics (Los Angeles, California), pp. 551–565.

PHILLIPS, O.M., 1957. On the generation of waves by turbulent wind. *Journal of Fluid Mechanics,* 2, 417–445.

PHILLIPS, O.M., 1958. The equilibrium range in the spectrum of wind-generated waves. *Journal of Fluid Mechanics,* 4, 426–434.

TORRENCE C. and COMPO, G.P., 1998. A practical guide to wavelet analysis. *Bulletin of the American Meteorological Society,* 79(1), 61–77.

YOUNG, I.R. and VERHAGEN, L.A.,1996a. The growth of fetch limited waves in water of finite depth. Part 1: Total energy and peak frequency. *Coastal Engineering,* 29, 47–78.

YOUNG, I.R. and VERHAGEN, L.A.,1996b. The growth of fetch limited waves in water of finite depth. Part 2: Spectral evolution. *Coastal Engineering,* 29, 79–99.

YOUNG, I.R. and VERHAGEN, L.A.,1996c. The growth of fetch limited waves in water of finite depth. Part 3: Directional spectra. *Coastal Engineering,* 29, 101–121.